



## Experimental investigation of the mechanical connection between FRP laminates and concrete

Roberto Realfonzo\*, Enzo Martinelli, Annalisa Napoli, Bruno Nunziata

Department of Civil Engineering, University of Salerno, Via Ponte don Melillo, 84084 Fisciano (SA), Italy

### ARTICLE INFO

#### Article history:

Received 6 February 2012

Received in revised form 10 April 2012

Accepted 13 May 2012

Available online 23 May 2012

#### Keywords:

A. Polymer–matrix composites (PMCs)

A. Laminates

B. Interface

C. Finite element analysis (FEA)

Experimental tests

### ABSTRACT

This paper presents the results of an experimental campaign aimed at investigating the interfacial behavior of Fiber Reinforced Polymer (FRP) laminates Mechanically Fastened (MF) to concrete members.

The experimental program includes 34 direct shear tests (DSTs) performed on FRP laminates fastened to concrete prisms through either single or multiple screwed anchors arranged according to different layouts.

In 17 tests a steel washer was interposed between the head of each fastener and the outer side of the laminate; in the remaining ones, instead, no washer was used.

The performed tests allowed to evaluate the behavior of the MF-FRP connections mainly in terms of load-carrying capacity, FRP strain distribution and damage mechanism; the influence on the experimental response of both fastener configuration and washer presence was also investigated.

Results of tests on specimens fastened by using a single screw were used for calibrating a possible force–displacement law to describe the interaction between MF-FRP laminate and concrete substrate.

Finally, simplified FEM models were implemented and verified for better simulating the experimental results and estimating the strain and stress distributions within the laminate.

© 2012 Elsevier Ltd. All rights reserved.

### 1. Introduction

The use of Mechanically Fastened Fiber Reinforced Polymer (MF-FRP) strips for the flexural strengthening of reinforced concrete (RC) members has been recently proposed as an alternative solution to the most common externally-bonded (EB-FRP) sheets and laminates [1–3].

This technology is based on employing pre-cured FRP laminates characterized by enhanced bearing strength and connected to the concrete substrate by means of shot or screwed steel anchors.

Attractive applications include emergency repairing of structures and infrastructures, where constructability and rapidity of installation are critical requirements.

The first applications of MF-FRP laminates were aimed at strengthening RC bridges and infrastructures [4,5].

Then, a number of experimental studies were performed around the world with the aim of investigating the performance of RC beams and slabs externally strengthened by MF-FRP laminate and quantifying the benefits obtained in terms of strength, stiffness and displacement capacity [2,3,6–9].

Published research has also highlighted the advantages of such technique in terms of ease of installation and preventing strip delamination before concrete crushing. A wide state of the art report covering the last 10 years can be found in [10].

The growing interest in the MF-FRP technique is confirmed by the ongoing development of pre-standard documents by ACI sub-Committee 440-F and RILEM Technical Committee 234-DUC.

Comparative experimental studies [11,12] on the static and fatigue performance of RC beams strengthened in bending by either MF- or EB-FRP laminates, showed that similar strength levels can be attained.

Some experimental investigations also examined the feasibility of connecting an FRP laminate to the concrete substrate by both adhesive and mechanical anchors (EB + MF-FRP system) [12–14].

One of the latest experimental investigations also showed that the MF-FRP system is viable for strengthening existing reinforced-concrete beams in shear [15]. The feasibility of this strengthening technique was widely demonstrated experimentally in the upgrading of two-way slabs [16].

More recently, MF-FRP laminates were also employed for enhancing the flexural capacity of wooden beams [17], while the application of this system to reinforce masonry walls under both in-plane and out-of-plane actions seems to be a promising prospective [18].

The fastener layout is a key aspect controlling the actual force–slip behavior at the MF-FRP laminates–concrete interface. The influence of different fastening patterns has been investigated by several authors [7–9]; they highlighted that the occurrence of interface slips due to the bearing in the laminate makes the estimate of the ultimate flexural capacity of MF-FRP strengthened beams difficult, as the assumption of “plane sections remaining plane” cannot be applied

\* Corresponding author. Tel.: +39 089 964085; fax: +39 089 968739.

E-mail address: [rrealfonzo@unisa.it](mailto:rrealfonzo@unisa.it) (R. Realfonzo).

anymore. Nevertheless, models currently available to predict the flexural response of MF-FRP strengthened RC members [1,19] all rely on the assumption of “perfect bond” between the concrete substrate and the FRP laminate thereby neglecting any possible slip.

To address this issue, the effect of the partial interaction between concrete and FRP laminate was recently studied by some authors [9,20–22], as it is more relevant for mechanically fastened than for externally bonded FRP [23].

Preliminary proposals for describing the relationship between the nominal bearing stress exchanged at the fastener-strip contact surface and the resulting FRP-concrete interface slip were published in the scientific literature for two types of fasteners (either shot or screwed) [24]. However, due to the lack of extensive analytical and experimental investigation, additional information on the interaction between fasteners, FRP strip and concrete is needed for formulating accurate and reliable design rules.

For this purpose, a wide experimental investigation has been recently completed at the Testing Laboratory for Materials and Structures of the University of Salerno consisting of 34 direct shear (DS) tests performed, in displacement control, on FRP laminates mechanically fastened to concrete prisms by means of screwed anchors.

With the aim to achieve a thorough knowledge of the interfacial behavior between concrete and FRP – which is a key point for simulating the structural response of RC members (either beams or slabs) externally strengthened by MF-FRP systems – the concrete block-laminate connections were realised by using either single or multiple fasteners arranged according to different layouts. For 17 tests the fastener installation was performed by using a steel washer between the head of the fastener and the outer side of the laminate; in the remaining ones, instead, the washer was never used.

The performed tests enabled to describe the behavior of the MF-FRP connections mainly in terms of load-carrying capacity, FRP strain distribution and damage mechanism; the beneficial effects due to the use of washers were also investigated.

Moreover, results of tests on specimens fastened by using a single screw were used for calibrating a constitutive model of the connection, i.e. the load–slip law able to simulate the FRP-concrete interfacial behavior. It is worth noting that a proper identification of the interfacial relationship represents a primary step for modeling the flexural behavior of MF-FRP strengthened beams, whose preliminary investigations are documented in [20].

Finally, simplified FEM models were implemented in the SAP2000 [25] code with the aim to better describe the experimental results and estimate the strain and stress distributions within the laminate.

## 2. Experimental program

The experimental program, carried out at the Testing Laboratory for Materials and Structures of the University of Salerno, includes a total of 34 direct shear tests performed, in displacement control, on FRP laminates mechanically fastened to concrete blocks by means of screwed anchors (Fig. 1a).

This paper presents the results of the whole experimental program. Emphasis is given on evaluating the behavior of the FRP-concrete interface by varying some key parameters, such as the number of fasteners and the spacing among them, and investigating the positive effects due to the clamping pressure applied by the washer placed between the head of the fastener and the outer side of the laminate.

The following sections report a detailed description of the test specimens and materials, strengthening layouts, test setup and instrumentation.

### 2.1. Test specimens, materials and strengthening layouts

Test specimens consists of pre-cured FRP laminates fastened to concrete prisms having a  $150 \times 200 \text{ mm}^2$  cross section; depending

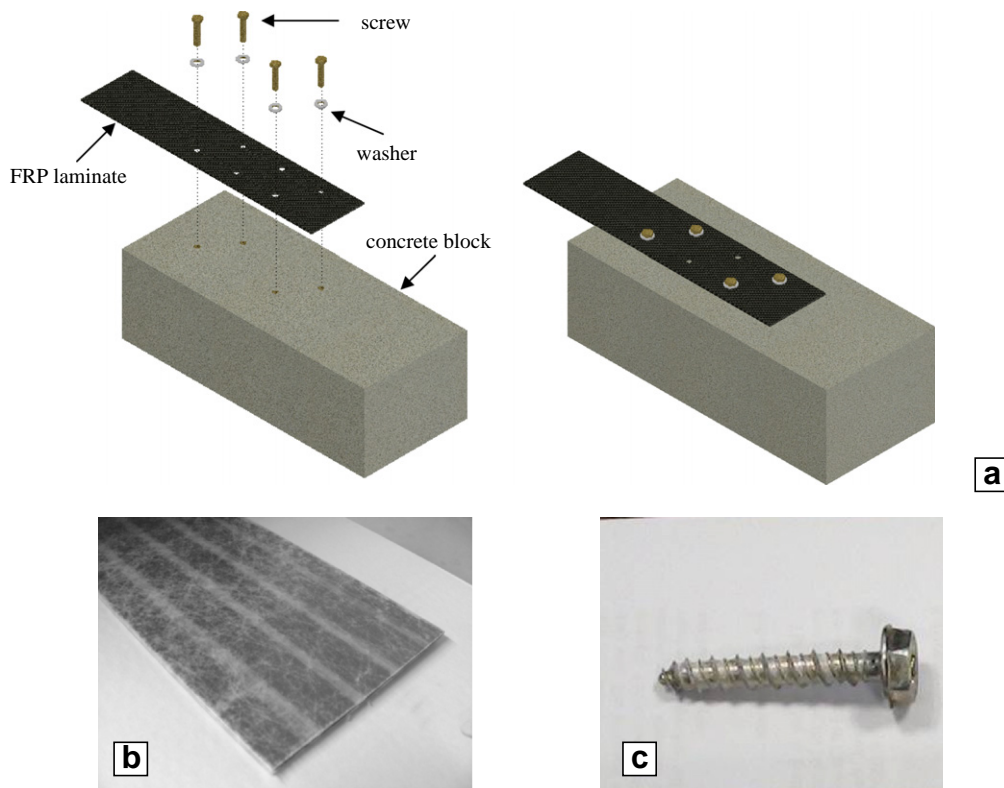


Fig. 1. Schematic of test specimens: (a) MF-FRP connection; (b) FRP laminate; (c) screw anchor.

on both the number and spacing of fasteners, the length of concrete blocks ranged from about 236 mm to about 400 mm.

The average value of the cylinder compressive strength ( $f_{cm}$ ) of the designed concrete mixture was equal to 25 MPa, with a standard deviation of 3.62 MPa. These values were obtained by testing in compression a set of 150 mm edge cubic samples, cast along with the prisms and cured under the same environmental conditions;  $f_{cm}$  was assumed equal to the 83% of the mean value of the cubic strength,  $R_{cm}$ .

The pre-cured laminates used for the MF-FRP system are shown in Fig. 1b; they were glass- and carbon-vinyl ester pultruded strips with enhanced transverse and bearing strength by means of embedded fiberglass mats [26].

Width and thickness of the laminates, denominated “SafStrip” by the manufacturer, were 102 and 3.2 mm, respectively. The average values of the mechanical properties of such linear-elastic FRP materials, as provided by the supplier [26], are listed in Table 1, where  $f_{fu}$ ,  $E_f$  and  $\epsilon_{fu}$  are the tensile strength, the elastic modulus and the ultimate strain in the longitudinal direction of the laminate, respectively;  $f_{uo}$  represents the open-hole tensile strength, whereas  $f_{ub}$  and  $f_b$  are the unclamped and clamped bearing strength, respectively.

It is highlighted that several researchers have performed extensive experimental investigations aimed at characterizing the mechanical properties of these laminates. Among them, Rizzo et al. [27] carried out many tensile and bearing tests, according to the respective ASTM Standards, with the aim to achieve a thorough knowledge of the mechanical behavior both in longitudinal and transverse direction of the FRP laminate. Therefore, further details about the meaning of the mechanical properties provided by the manufacturer are available in [27].

Screw steel anchors were used to fasten the FRP laminate to concrete (Fig. 1c). The anchors, driven into pre-drilled holes using a common torque wrench, had a 45 mm shank length and a 6 mm diameter [28].

In order to investigate the feasibility of the easiest and most practical MF-FRP installation, gap fillers (resin) were never introduced in the pre-drilled holes.

In 17 tests, additional washers, having an outer diameter of 32 mm, were used with each fastener in order to exploit the two-fold advantage: (1) increase the bearing strength by providing a clamping pressure on the larger area of the FRP strip around the fastener (which minimizes any possible slip between the fastener and the FRP strip); (2) reduce the damage in the FRP caused, during tests, by the fastener head rotation under high levels of the imposed displacement.

Fig. 2 shows the five fastener layouts (labeled “1”, “2A”, “2B”, “4A” and “4B”) selected for this study. Except for the layout “1”, where the fastening is realised with a single connector, the other configurations are characterized by the use of multiple fasteners (two fasteners for the layouts “2A” and “2B” and four fasteners for the “4A” and “4B” ones).

In these configurations, the FRP laminate has two staggered rows of fasteners, spaced at about 51 mm, which allow for an optimal diffusion of normal stresses throughout the laminate width and are aimed at minimizing shear lag effects observed by using a single row of fasteners [1,7].

As it can be observed in Fig. 2, the layouts “2A”–“2B” and “4A”–“4B” are characterized by different fastener spacing; in particular, in the layouts “2A” and “4A” the spacing between two consecutive fasteners is always equal to 38 mm, while in the layout “2B” is equal to 114 mm. In the layout “4B”, instead, it varies from 38 mm to 114 mm.

The edge distance of 65 mm, used in all configurations, was selected to offset the likelihood of laminate cleavage-tension failure [1], and to prevent shear-out failure at the outermost fasteners [7].

Finally, it is mentioned that, among the five configurations shown in Fig. 2, the layouts 4A–4B were already investigated in a previous experimental campaign performed on RC slabs strengthened in flexure with MF-FRP laminates [8,20].

**Table 1**  
Mechanical properties of the FRP laminates.

$f_{fu}$ (MPa)	$E_f$ (GPa)	$\epsilon_{fu}$ (%)	$f_{uo}$ (MPa)	$f_{ub}$ (MPa)	$f_b$ (MPa)
852	62	1.36	652	214	351

2.2. Test set-up

Fig. 3 shows a schematic of the setup designed to assure direct shear at the FRP–concrete interface.

Tests were performed in displacement control with a rate of 0.05 mm/s by using a 600 kN Schenck universal testing machine. As observed from the figure, the specimens were first restrained within two stiff end steel plates (upper and lower ones) by pre-tensioning four high strength threaded rods having a 20 mm diameter, and then were placed into the tensile loading frame.

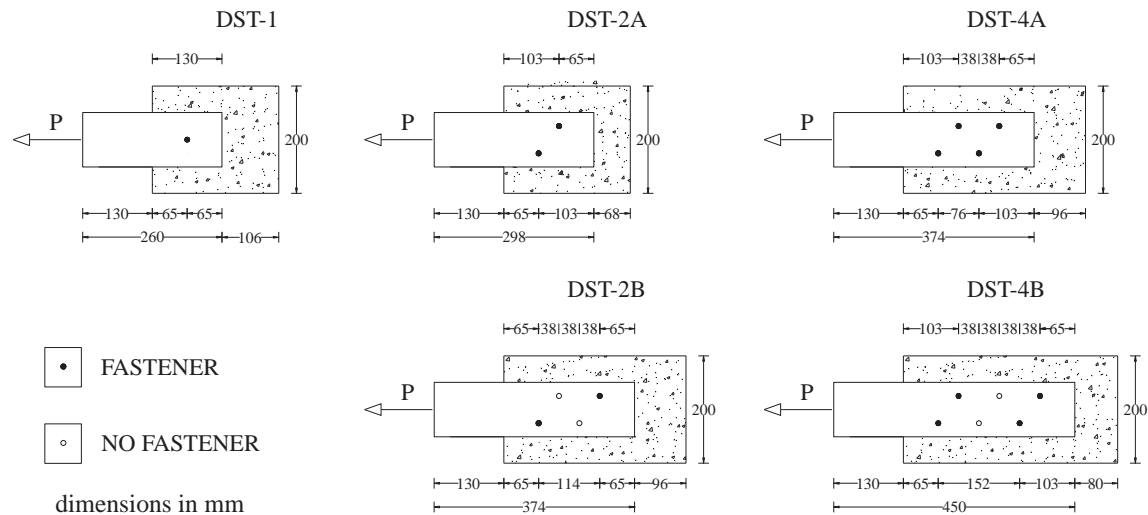


Fig. 2. Fastener layouts.

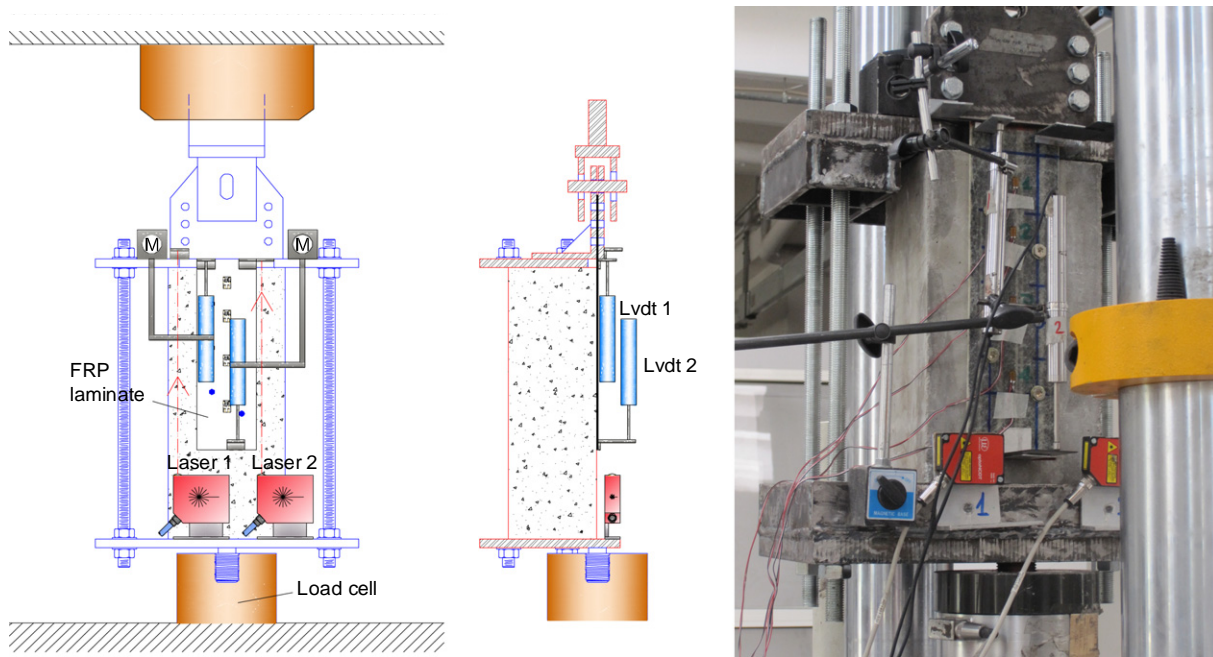


Fig. 3. Test setup and instrumentation.

An anchorage length of the FRP laminate, equal to about 130 mm, was always adopted to assure the proper gripping of such a laminate within the tensile machine. In particular, the gripping was realised by restraining the laminate between two steel plates; these were then tightened with six high strength bolts using a small torque wrench. In order to increase the laminate-plate friction, the inner surface of such steel elements was made rough.

The specimens were properly instrumented with laser sensors (see laser 1 and laser 2 in Fig. 3) and linear variable displacement transducers (see LVDT 1 and LVDT 2) to monitor laminate displacements at both free and loaded ends, and any possible differential displacements (“slip”) occurring at the gripping system. In particular:

- Laser 1 monitored the total displacement imposed by the testing machine ( $s_{tot}$ ), i.e. the displacement obtained by adding the laminate-concrete slip at loaded end ( $s_l$ ) and the possible laminate-plates slip at gripping system ( $\Delta_s$ );
- Laser 2 measured the displacement  $s_l$  (which also accounted for the potential deformability of the several test set-up components, i.e. steel plates, rods and concrete prism);
- LVDT 1 monitored the “net component” of  $s_l$ , i.e. without accounting for the abovementioned deformability of the test set-up components;
- LVDT 2 measured the relative laminate-concrete slip at the free end ( $s_f$ ), which also coincided with the displacement exhibited at the fastener located furthestmost from the loaded end.

Several strain gauges, 10 mm in length, having a resistance of  $350 \pm 0.6\%$  and a gauge factor of  $2.095 \pm 0.5\%$ , were used to measure the strains along the FRP strip during tests.

Fig. 4 depicts the typical strain gauges arrangement adopted for the test layouts.

All instruments were connected through a master panel to a data acquisition system. The imposed displacement and the corresponding load were recorded as an output of the testing machine. The latter was also monitored by a 400 kN load cell placed below the steel base plate and restrained to the lower cylindrical element of the testing machine. This cell, having the maximum capacity

lower than the threshold characterizing the Schenck machine, assured to monitor the loads expected from the experimental tests with greater accuracy.

The acquisition system was set to continuously scan the instruments during testing and to save the raw data to a file at intervals of 0.5 s (i.e. two measures recorded per second).

### 3. Test results

Table 2 summarizes relevant results of the thirty-four tests included in the experimental campaign.

The first set of 17 tests refers to FRP laminates fastened to concrete blocks using screws without washers, while the second one refers to 17 companion specimens provided with washers.

Tests are labeled as “DST- $xw(y)$ ”, where “ $x$ ” refers to the layout definition represented in Fig. 2 (i.e. “ $x$ ” = 2A, 2B, 4A or 4B); the character “ $w$ ” (if any) denotes specimens in which a washer was placed between the head of the anchor and the outer side of the laminate, whereas “ $y$ ” indicates the  $y$ -th test of the same layout (i.e. “ $y$ ” = a, b, c or d).

In detail, Table 2 reports: the number of fasteners ( $N_F$ ); the peak axial load ( $H_{max}$ ) and the corresponding slip measured at free ( $s_{f,max}$ ) and loaded ends ( $s_{l,max}$ ) of the laminate; the slip at free ( $s_{f,85\%}$ ) and loaded end ( $s_{l,85\%}$ ) calculated on the monotonic envelope in correspondence of 15% strength degradation (i.e. at a conventional collapse); the ultimate values of the load ( $H_u$ ) and slips ( $s_{f,u}$  and  $s_{l,u}$ ) exhibited by specimens when tests were stopped.

From the table, it has to be noted that:

- (a) some displacement data at 85%  $H_{max}$  are missing due to premature fastener rupture experienced during the tests or because measure devices stopped working prematurely;
- (b) for some tests it was found that the displacement data (marked in *italics* in the table) recorded at free end of the laminate by measure devices were slightly greater than the corresponding values obtained at the loaded end. However, such anomaly does not affect the quality of the results obtained from the overall experimental campaign.

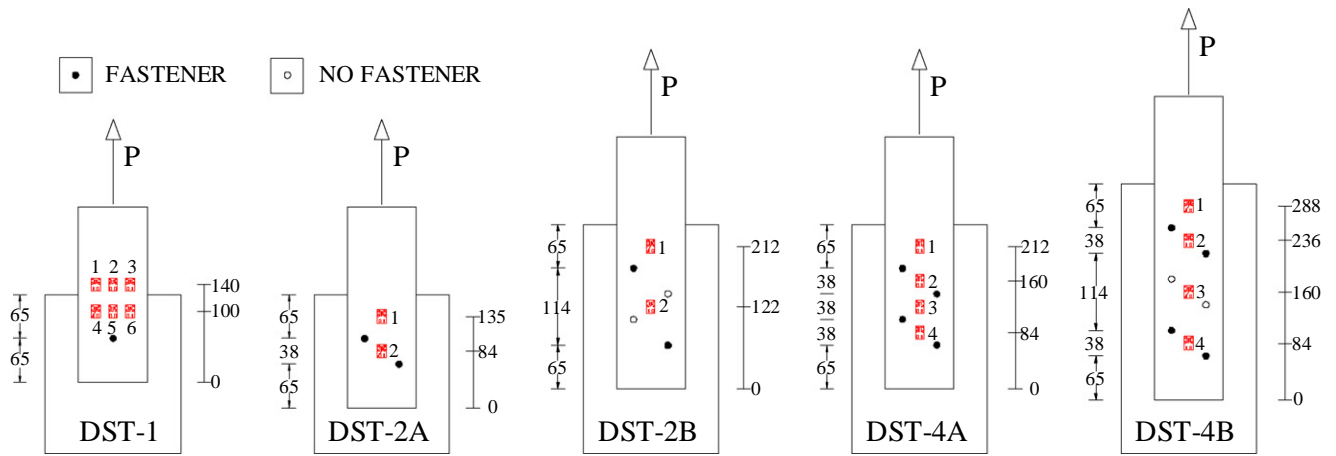


Fig. 4. Typical arrangement of strain gauges along the FRP laminate.

Table 2  
Test results of MF-FRP connections.

	$N_F$	Test	$H_{max}$ (kN)	$s_{f,max}$ (mm)	$s_{l,max}$ (mm)	$s_{f,85\%}$ (mm)	$s_{l,85\%}$ (mm)	$H_u$ (kN)	$s_{f,u}$ (mm)	$s_{l,u}$ (mm)
Fasteners w/o washer	1	DST-1(a)	11.6	9.16	9.66	11.46	12.35	6.3	18.56	20.25
		DST-1(b)	10.8	12.41	12.00	13.95	14.45	4.1	26.37	26.85
		DST-1(c)	12.7	4.83	5.62	6.15	6.90	4.7	13.00	13.61
		DST-1(d)	10.5	7.89	8.34	10.57	11.02	4.2	20.20	19.97
	2	DST-2A(a)	27.5	11.97	16.81	13.30	18.95	12.8	18.52	21.85
		DST-2A(b)	17.9	7.41	6.72	10.08	10.20	7.4	20.49	22.93
		DST-2A(c) <sup>a</sup>	21.3	7.36	8.21	–	–	21.3	7.36	8.21
		DST-2A(d)	21.1	7.09	6.66	8.58	9.02	7.7	18.04	15.86
	4	DST-2B(a)	29.7	11.24	11.77	13.40	14.10	13.4	22.00	23.69
		DST-2B(b)	23.4	5.98	6.37	10.10	10.12	7.2	19.56	20.31
		DST-2B(c)	25.7	8.62	8.68	13.15	16.05	9.1	20.79	26.34
		DST-4A(a)	55.9	13.81	14.21	17.60	18.70	24.6	25.75	26.55
	4	DST-4A(b)	35.9	11.40	13.42	15.35	18.10	20.1	24.17	27.19
		DST-4A(c)	40.0	13.96	12.55	15.40	14.90	25.1	18.88	19.26
		DST-4B(a)	46.0	11.46	13.39	16.70	18.35	26.1	20.71	22.40
		DST-4B(b)	38.0	11.63	13.75	13.55	15.80	8.5	30.28	32.18
Fasteners w/ washer	1	DST-4B(c)	41.4	6.45	9.08	9.60	11.70	10.1	24.18	26.51
		DST-1w(a)	13.1	14.82	16.39	23.15	24.35	5.5	31.34	32.73
		DST-1w(b)	13.2	23.25	24.43	29.65	29.40	7.6	34.16	36.77
		DST-1w(c)	14.0	17.80	17.74	26.80	24.30	4.1	37.32	37.93
	2	DST-1w(d)	11.8	16.87	18.00	30.40	30.60	4.8	35.19	34.62
		DST-2Aw(a)	24.0	17.40	17.91	33.80	32.10	18.5	35.54	34.21
		DST-2Aw(b)	31.2	17.13	18.25	21.45	25.35	18.9	29.64	34.14
		DST-2Aw(c) <sup>a</sup>	28.5	7.98	8.77	–	–	–	–	–
	4	DST-2Bw(a)	26.5	12.25	12.53	16.60	17.58	16.7	26.86	30.25
		DST-2Bw(b)	30.1	16.59	18.11	23.10	25.20	16.5	29.18	30.82
		DST-2Bw(c)	30.1	12.85	14.56	23.59	25.73	14.4	29.90	35.12
		DST-4Aw(a)	53.9	17.71	19.07	24.45	24.50	38.3	30.91	29.85
	4	DST-4Aw(b) <sup>a</sup>	51.9	17.36	17.70	–	–	–	–	–
		DST-4Aw(c) <sup>b</sup>	51.3	10.51	10.95	–	15.80	46.1	–	26.95
		DST-4Aw(d)	51.0	14.80	15.09	22.49	22.51	30.0	28.19	28.51
		DST-4Bw(a) <sup>a</sup>	57.8	19.58	19.19	–	–	–	–	–
4	DST-4Bw(b)	57.3	14.89	15.48	23.40	22.91	41.7	27.70	26.98	
	DST-4Bw(c) <sup>b</sup>	59.3	14.35	14.92	–	–	53.85	16.49	17.62	

<sup>a</sup> Some displacement data at 85%  $H_{max}$  are missing due to premature fastener rupture.

<sup>b</sup> Some displacement data at 85%  $H_{max}$  are missing as the measure devices stopped working prematurely.

Fig. 5 depicts, for a representative test, the experimental responses  $H-s_l$  and  $H-s_f$  obtained by measuring slips with LVDT1 and LVDT 2, respectively. It has to be noted that the differences between displacements  $s_l$  and  $s_f$  measured with the two LVDTs provide the elastic elongation of the FRP strip.

In all tests the slip  $\Delta_s$  measured between FRP laminate and steel plates of the machine's gripping system, was always found to have a negligible effect.

The experimental tests showed that bearing developing at the contact surface between FRP laminate and steel anchor actually controls the force capacity of the structural system under consideration. As expected, in the case of DS tests with multiple fasteners, the bearing developed firstly closest to the loaded end of the laminate and, subsequently, engaged the remaining ones.

Furthermore, the damage mechanisms were strongly influenced by the fastener head rotation which was mitigated by the washer.

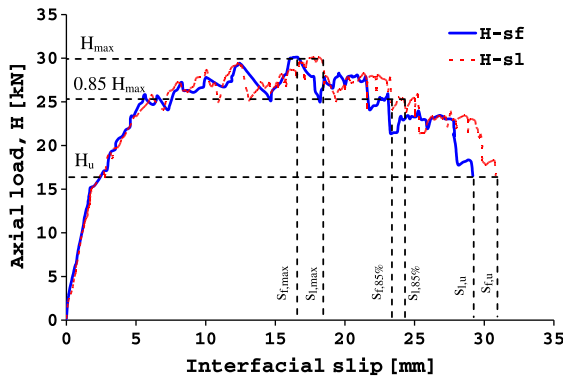


Fig. 5. Load-displacement curves: test DST-2Bw(b).

Details on the failure modes and on the main results obtained from the performed tests are reported in the following sections.

### 3.1. Laminate-concrete connection with one fastener

The performed tests clearly showed that the introduction of a washer significantly affects the behavior of an FRP-concrete connection in terms of strength and mainly of ductility. As expected, applying a clamping pressure on a greater area of the strip around the fastener, the bearing strength of the plate improves and, consequently, the connection keeps the load carrying capacity up to higher levels of imposed displacement. More details about the positive effects due to the clamping action can be found in [29].

In order to better understand the differences of the behaviors observed during “DST-1” and “DST-1w” tests, Fig. 6 depicts the typical damage phenomena characterizing fastened connections realised either in absence (Fig. 6a and b) or in presence (Fig. 6c and d) of washer.

As noted, in both types of tests, the dominant damage was characterized by the bearing in the FRP plate. However, in the case of “DST-1” specimens, the bearing at fastener location was early followed by a progressive damage of the outer surface of the FRP strip (Fig. 6a and b).

This punching of the laminate, emphasized by the absence of the washer, was caused by the rotation of the screw head that tends to move below the laminate with a subsequent reduction of the connection capacity (Fig. 6a).

Fig. 6b shows the bearing damage of the FRP laminate and the deformation in bending exhibited by the fastener at the end of test.

In the case of “DST-1w” tests, instead, the use of washers prevented the laminate from being prematurely damaged by the screw head; in fact, the occurrence of this phenomenon was limited to high levels of interfacial slip, where the fastener rotation

caused the bending of the washer and then the FRP material removal (Fig. 6c and d).

The beneficial effects of washers can also be noted by observing Fig. 7 where the experimental tensile load-free end slip ( $H-s_f$ ) responses exhibited by four identical “DST-1” specimens (Fig. 7a) and four “DST-1w” ones (Fig. 7b) are plotted. It is relevant to mention that the displacements reported in the two figures were measured by a LVDT at the free-end of the FRP laminate; therefore, these values are not influenced by the elastic strains experienced at the loaded end.

From the above mentioned figures it can be noted that the experimental curves are all characterized by a rigid branch up to a load value of 1.5–2.0 kN, when the bearing in the FRP plate starts. After this threshold, the response of “DST-1” specimens significantly diverges from that shown by “DST-1w” ones.

In particular, the positive effects produced by the presence of washers lie in the higher displacements values exhibited at the achievement of the peak axial load and, predominantly, during the whole post-peak phase. In fact, unlike the significant softening branch characterizing the post-peak response of “DST-1” specimens, in presence of washers the maximum load kept approximately constant for a wide range of increasing values of the interfacial slip.

The performances of the MF-FRP connections having only one screw can also be examined by comparing the experimental results reported in Table 2. As observed, using the washer slightly improves the strength of the connection; in fact, the mean value of the peak loads calculated for “DST-1w” curves, equal to about 13 kN, is only 14% greater than the corresponding one computed for “DST-1” specimens which is about 11.4 kN.

Conversely, the average value of  $s_{f,max}$  (=18.2 mm) is almost twice higher than the respective result obtained for the tests w/o washer (=9.82 mm). This improved behavior in the case of “DST-1w” specimens is even more evident at the achievement of the conventional collapse where the average value of  $s_{f,85\%}$  (=27.5 mm) is 2.2 times greater than the corresponding one (=12 mm) computed for “DST-1” members.

However, it is highlighted that the displacements  $s_f$  exhibited by the specimen DST-1(c) were not considered in evaluating the average values as the experimental response of such member was rather different from that experienced by the other companion members.

Finally, it has to be underlined that at the end of all performed tests only a slight concrete crushing was observed at the fastener location.

### 3.2. Laminate-concrete connection with multiple fasteners

During the tests, MF-FRP connections realised by using multiple fasteners, w/ or w/o washer, exhibited damages very similar to



Fig. 6. DST-1 (a and b) and DST-1w tests (c and d): main damage mechanisms.

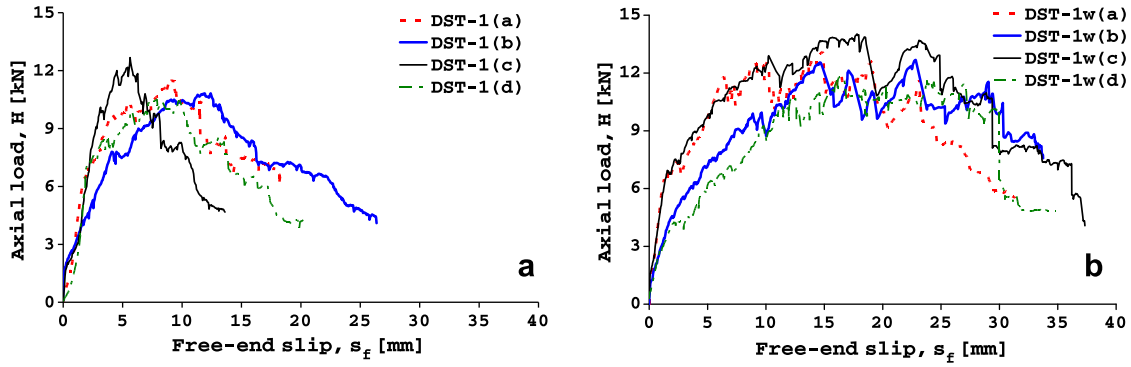


Fig. 7. Load-slip curves of connections realised using one fastener: without washer (a); with washer (b).

those observed in the case of “DST-1” and “DST-1w” specimens: the bearing deformation activated since the initial step of loading and first developed at hole location closest to the loaded end of the laminate; the absence of washers prematurely increased the damage in the FRP because of the progressive rotation of the fasteners which tried to punch the laminate.

Fig. 8 collects some pictures taken at the end of the performed tests: the bearing damage in the FRP laminate is always clearly showed.

The key role played by some detailing (i.e. the presence of washers; the fastener spacing) on the performance of MF-FRP connections can be well understood by observing Fig. 9; the figure shows the load-free end slip ( $H-s_f$ ) responses exhibited by all specimens with two fasteners and four fasteners.

In particular, Fig. 9a and c refers to MF-FRP connections where screws without washer were installed according to layouts 2A–4A and 2B–4B, respectively, whereas Fig. 9b and d refers to companion specimens equipped with washers.

Disregarding the influence of the fastener layout, it is observed that the force-displacement curves obtained from tests w/o washer are affected by a significant level of variability even in the case of similar specimens. Conversely, specimens having anchors w/ washer exhibited a more regular behavior and companion specimens responded in a substantially similar way.

The data dispersion in tests on specimens without washers, further confirmed from the results reported in Table 2, implies that uncertainties related to fastener installation (i.e. making holes in the laminate not larger than the fastener diameter; keeping a perfect uprightness when drilling holes in the concrete and tightening the anchors; checking the applied clamping torque when installing the fasteners, etc.) may significantly affect the performance of a MF-FRP connection. In this regard, the presence of washers and their action on the laminate is expected to reduce such uncertainties.

Furthermore, for a given fastener layout, test specimens using washer always experienced, on the average, a non-negligible increase of strength over the corresponding connections not provided with washer. This is even more evident in the case of laminates connected to the concrete substrate with four fasteners: tests DST-4Aw and DST-4Bw have experienced an average increase of the peak load equal to about 37% and 39%, respectively, with respect to the corresponding specimens DST-4A and DST-4B. It is highlighted that the specimen DST-4A(a) was not considered in the comparison as it exhibited a load-slip response significantly dissimilar from those obtained for companion identical specimens (see Fig. 9a).

In particular, when using the washer, the maximum tensile force is as high as the number of fasteners; for instance, the peak load almost doubles as the number of fasteners increases from 2 to 4.

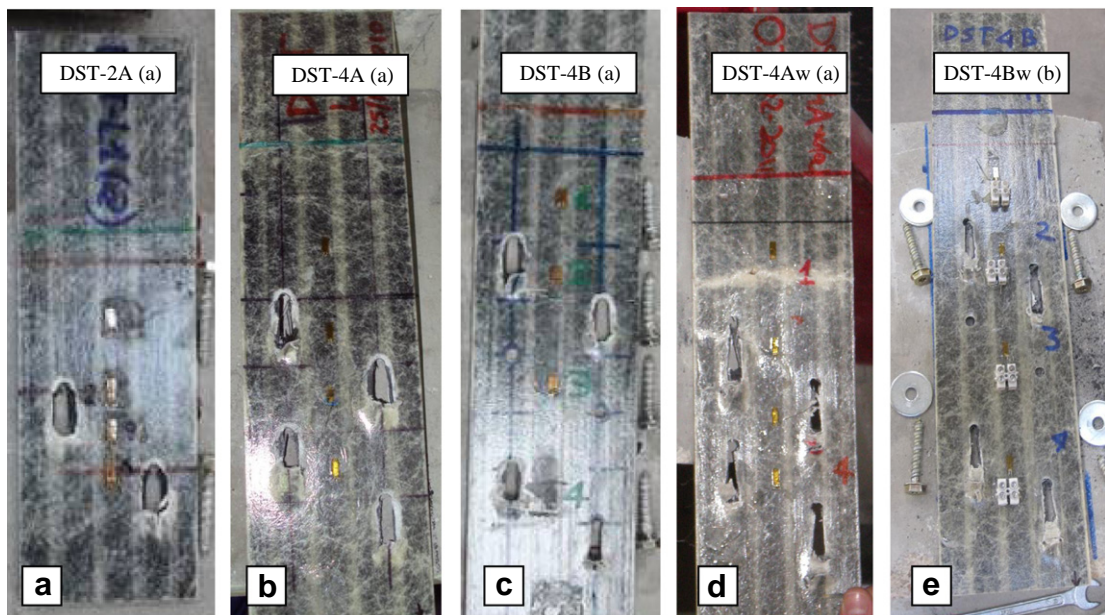


Fig. 8. Bearing damage of the FRP in the case of: fastener w/o washer (a–c); fastener w/ washer (d and e).

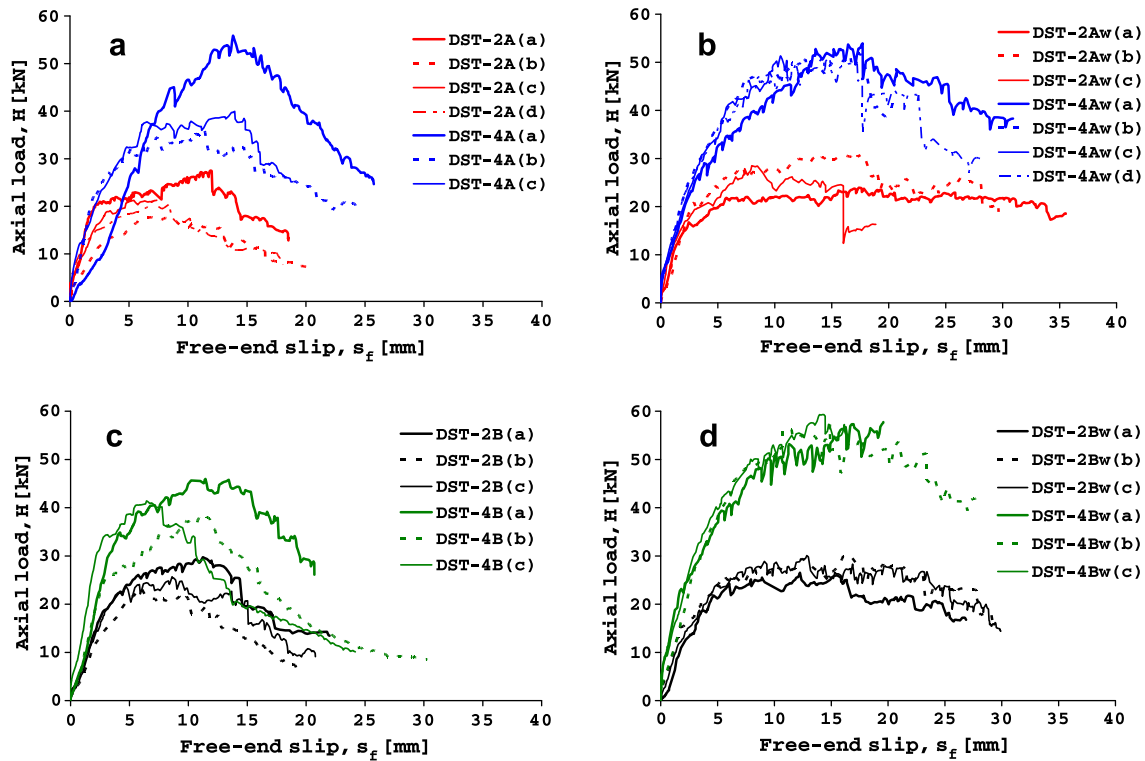


Fig. 9. Experimental load-slip relationships in the case of multiple fasteners: test series w/o washer (a and c); test series w/ washer (b and d).

The beneficial effects due to the use of a washer are even more evident in terms of higher displacements values exhibited at the achievement of the peak axial load and, predominantly, during the whole post-peak phase. This improved behavior is again due to delayed occurrence of the fastener head rotation which in turn restricted the laminate damage only to high levels of interfacial slip.

Conversely, the post-peak response of connections without washer is characterized by a remarkable softening branch which early leads to a faster achievement of the conventional collapse.

It was found that tests DST-4Aw and DST-4Bw produced an average increase of the free-end slip  $s_{f,85\%}$  equal to about 52% and 76% with respect to the corresponding specimens DST-4A and DST-4B. Similar results were found by considering the value of  $s_f$  at the achievement of the peak axial load  $H_{max}$ .

Finally, besides both washer and fastener spacing, Fig. 9 shows that, by neglecting the specimen DST-4A(a), the behavior of the connections with four anchors is characterized by an increase of the initial stiffness over the corresponding specimens with two screws.

The influence of the fastener spacing can be better investigated by observing Fig. 10 where the comparisons between layouts 2A–2B (Fig. 10a and b) and layout 4A–4B (Fig. 10c and d) for fasteners installed w/ and w/o washer are plotted.

As noted, the fastener spacing plays a more relevant role in the case of tests w/o washer where, except for some tests, a better performance in terms of initial stiffness, strength and ductility, is associated to anchors with larger spacing (layout “B”), thus confirming what already found in other experimental investigations [5,8].

#### 4. A bearing stress–interface slip model

The interfacial behavior between concrete and FRP laminate significantly affects the overall performance of MF-FRP strengthened members. Therefore, an appropriate relationship able to correctly describe such interaction has to be developed.

To this purpose, in a first study, Napoli et al. [20] implemented a numerical model for simulating the flexural response of MF-FRP strengthened members. The finite-element procedure included two non-linear constitutive models for FRP-concrete interface: the bearing stress–slip relationship proposed by Elsayed et al. [24] and a simplified (bilinear) one suggested by the authors. The comparison between experimental results and numerical predictions showed: a satisfactory agreement when using the accurate model; a more conservativeness of the simulated response using the simplified law, making it suitable for design purposes.

Later, Martinelli et al. [21] proposed a numerical modeling to reproduce the behavior of MF-FRP strips in direct shear test conditions. Such modeling was used within the framework of an inverse procedure for identifying a more refined constitutive law of the connection.

The inverse procedure – originally formulated for bonded FRP-strips [30] – was then applied by considering both the results from DS tests performed by Elsayed et al. and the first results from tests carried out by the authors [31].

A comprehensive study on the application of this numerical modeling has been recently documented in [32].

In the following, two tri-linear  $H-s_f$  interfacial relationships, suitable for connection made w/ and w/o washer, are presented. The meaning of the six relevant parameters featuring these tri-linear constitutive laws ( $s_{f,b}$ ,  $H_b$ ,  $s_{f,max}$ ,  $H_{max}$ ,  $H_u$ ,  $s_{f,u}$ ) is better clarified by Fig. 11.

Five of them were calibrated by best-fitting, through least-square regression analyses, the experimental data from tests “DST-1w” and “DST-1”; the obtained values are listed in Table 3. The ultimate displacement  $s_{f,u}$ , instead, has been assumed equal to the lowest one between those obtained for each of the “DST-1” and “DST-1w” test sets (see Table 2).

Tests DST-1(c) and DST-1w(d) were not considered in the regression analyses since they behaved rather differently from the other analogous tests.

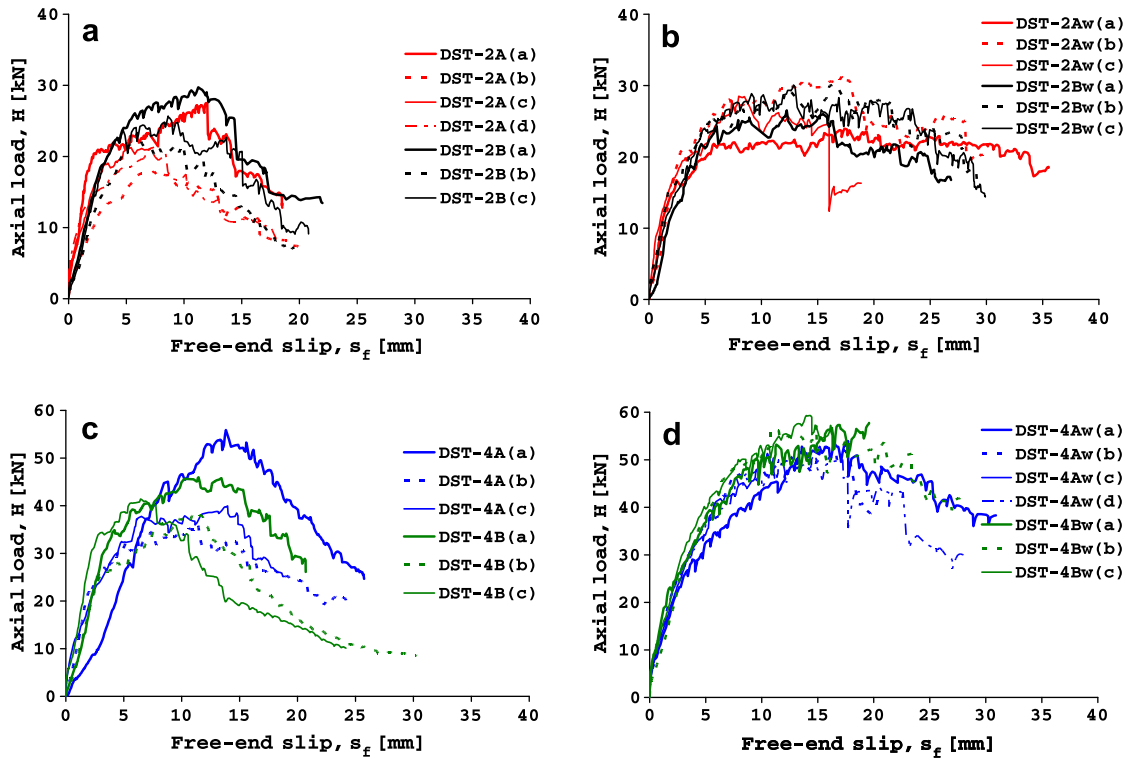


Fig. 10. Influence of the fastener layouts: test series w/o washer (a and c); test series w/ washer (b and d).

Comparisons between the experimental curves and the calibrated models are depicted in Fig. 12a and b.

In Fig. 13, the two best-fit relationships are represented in terms of bearing stress–slip laws and compared with the corresponding one identified by Elsayed et al. [24]; the latter was obtained by best-fitting results from DS tests on specimens made of the same FRP laminate considered herein, and fastened to the concrete with screws of 4.76 mm diameter, provided with a 16 mm washer [24].

The three relationships exhibit a very different response in terms of strength but similar initial stiffnesses.

The last consideration is relevant when modeling the flexural behavior of MF-FRP strengthened RC beams, where the values of the interfacial slips at connector location are of few millimeters (i.e. much lower than those experienced from DS tests) [20]. This implies that, apart from particular cases, in the carrying out a numerical modeling of strengthened beams: any of the three analytical laws can be considered; the beneficial effects by using washers may result not fully exploited.

The best-fit law by Elsayed et al. provides a conservative value of the maximum bearing strength; particularly, the plastic

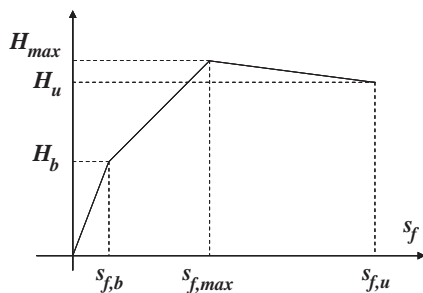


Fig. 11. Proposed axial load–slip model for screwed fastener w/ and w/o washer.

Table 3

Results of the best fit analyses performed by considering the interfacial model of Fig. 12.

Washer	$s_{f,b}$ (mm)	$H_b$ (kN)	$s_{f,max}$ (mm)	$H_{max}$ (kN)	$s_{f,u}$ (mm)	$H_u$ (kN)
No	2.59	7.3	9.00	10.8	18.55	5.9
Yes	1.81	6.8	14.88	13.1	31.30	8.2

threshold is approximately one-half of the maximum capacity computed for a DST-1w specimen (see Fig. 13).

It has to be underlined that the reduced strength found by Elsayed et al. is only partially justified by differences noted in the screw diameters (6 mm vs 4.76 mm, with a ratio between them of 1.26); therefore, differences highlighted between these interfacial models may be attributed also to: the shank length (45 mm vs 37 mm) of the connectors; the diameter (32 mm vs 16 mm) of the respective washers; the concrete strength level (25 MPa vs 42.1 MPa), that may affect the efficiency of driving the connector into pre-drilled holes.

Therefore, further investigation is needed to evaluate the influence of these factors on the concrete-FRP interface behavior; within this topic, a preliminary study was undertaken by Rizzo [5].

### 5. FEM model

The two relationships shown in Fig. 12 were employed within simplified FEM models developed for: (a) simulating the experimental responses of MF-FRP connections with multiple screws; (b) investigating the effect induced by staggered anchor patterns on the axial stress regime; (c) comparing the FRP strains obtained by the numerical simulations with those measured during the experimental tests.

The FEM models were generated by using the “SAP2000” computer programme [25].

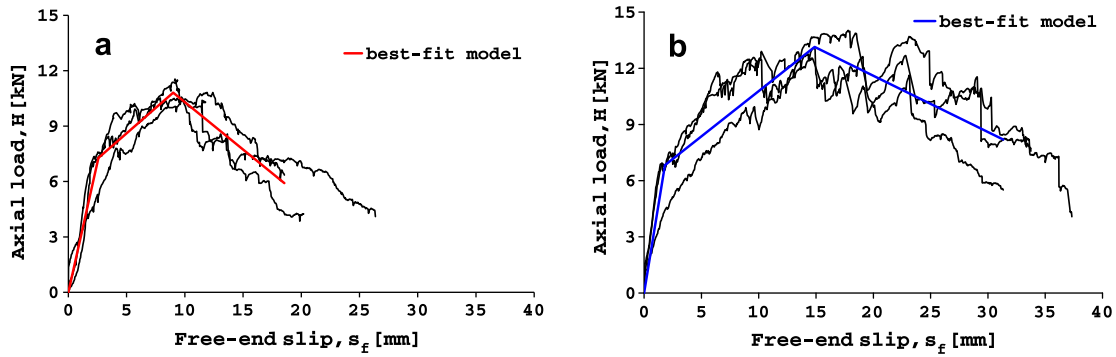


Fig. 12. Experimental load-slip curves and best-fit models for fastener w/o washer (a) and w/ washer (b).

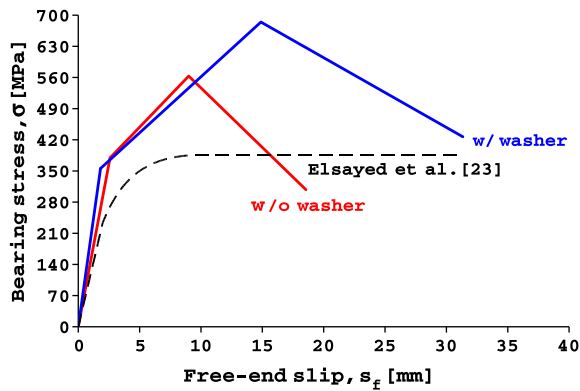


Fig. 13. Comparison between best-fit models obtained for the case of fastener w/o and w/ washer.

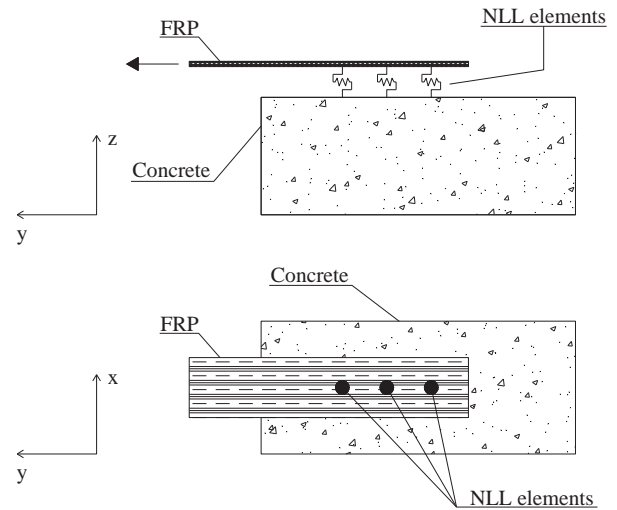


Fig. 14. Schematic of the FEM model.

The behavior of the FRP laminate was simulated through an assemblage of  $n$  “shell-thin” elements with  $5 \times 5 \text{ mm}^2$  area section; the number  $n$  ranged case by case depending on the length of the laminate employed in each test.

For the purposes of these numerical analyses it was considered possible to ignore the orthotropic nature of the laminates. Therefore, the FRP “SafStrips” have been considered as isotropic laminates, characterized by a longitudinal modulus of elasticity ( $E_f$  in Table 1) equal to 62 GPa (i.e. that provided by the manufacturer) and by a shear modulus ( $G_f$ ) ranging from 3 to 5 GPa.

The interaction between MF-FRP laminate and concrete was simulated by introducing a non-linear link element (NLL element) connecting two joints, one on the laminate and one on the concrete surface, at each fastener location. A schematic of the adopted model is depicted in Fig. 14.

The used link element (a “multi-linear elastic” support type) restrains vertical displacements of the laminate (i.e. along the  $z$ -axis), whereas along the  $x$  and  $y$  axes its behavior relies on one of the constitutive laws between those proposed in Section 4 (see also Fig. 12).

It is worth noting that the proposed FEM models are based on a simplified representation of the observed kinematic behavior: in the real behavior, as a result of the progressive bearing damage, the application point of the screw reaction moves through the time from an initial to a final position; in the model, instead, the NLL element reaction is steadily applied in the joint of the laminate where the link is assigned. Fig. 15 better highlights the differences existing between the simplified FEM model and the actual behavior.

To account for the effect of the laminate-screw relative displacements, the numerical analyses were performed on three slightly different models:

- in the first one (model 1), NLL elements were placed at the “initial” (i) fastener locations, which are defined by the layouts shown in Fig. 2;
- in the second one (model 2), instead, each link was shifted in a “final” (f) position, i.e. in the position of the fastener at the end of each test;
- in the third one (model 3), the FRP-concrete interaction at each fastener location was simulated by setting three link elements (NLL1, NLL2 and NLL3) at three different locations corresponding to the “initial” position (i), the “intermediate” position (i-f) and the “final” position (f), respectively (see Fig. 16a). The force-slip constitutive relationships of such three links (Fig. 16b–d) correspond to the three branches of the whole  $H$ - $s_f$  constitutive relationship represented in Fig. 16e.

Several simulations of experimental tests were performed by using the implemented FEM models.

Each simulation was performed by running a non-linear static analysis in displacement control; in particular, the same  $y$ -displacement was imposed to all the joints placed at the loaded end of the laminate (control nodes),

The analyses were performed by considering both  $G_f = 3 \text{ GPa}$  and  $G_f = 5 \text{ GPa}$ , in order to estimate the influence of the shear modulus on the stress distribution inside the FRP laminate.

Fig. 17 shows the comparison between the experimental axial strain results measured for the specimen DST-1w(c) (strain gauges

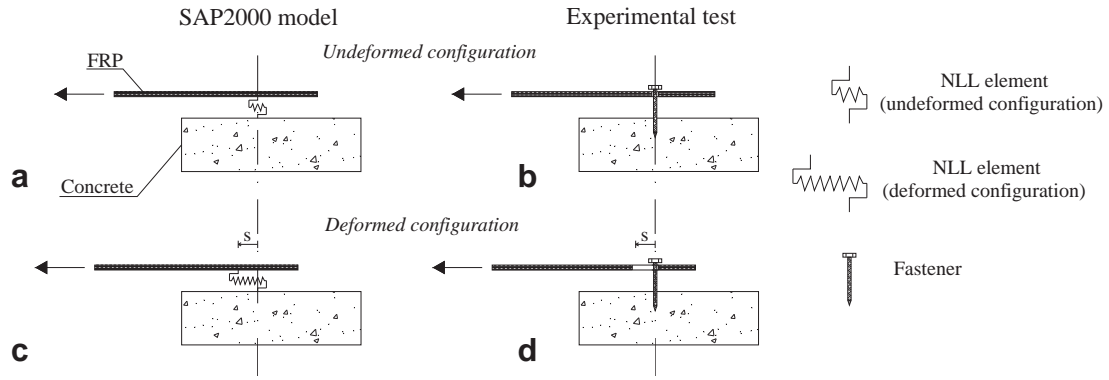


Fig. 15. Differences between the simplified FEM model (a and c) and the behavior experimentally observed (b and d).

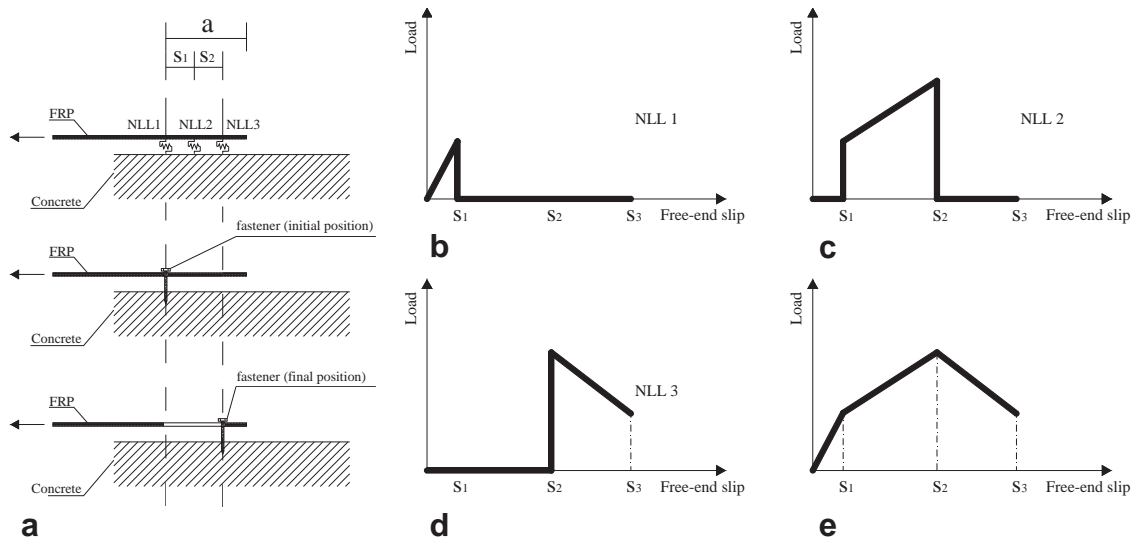


Fig. 16. Schematic of the model 3 realised by using three NLL elements.

2 and 5) and the numerical values obtained considering model 1 through 3, both plotted as a function of the imposed displacement.

It is highlighted that Fig. 17a reports the numerical results obtained by using a shear modulus  $G_f$  equal to 3 GPa, while strain depicted in Fig. 17b were found by considering  $G_f = 5$  GPa.

The location of the strain gauges 2 and 5 is shown in Fig. 17c. It is worth noting that the numerical results refer to strains computed on the mid-plane of the laminate, whereas the experimental readings were recorded by strain gauges placed on its outer surface. Therefore, discrepancies between models and experimental observations, mainly recognizable in the case of gauge 2, are also due to this aspect.

The comparisons reported in Fig. 17 allow to draw the following considerations:

- (a) although based on a simplified modeling of the FRP-concrete interaction, the simulations give rise to numerical strain values that match quite well the experimental data;
- (b) the model 3 better reproduces the variability of the experimental measures; strain values obtained by this model are intermediate between those given by models 1 and 2;
- (c) the shear modulus plays a significant role on the strain/stress regime developing within the FRP laminate; increasing the value of  $G_f$  from 3 to 5 GPa leads to a reduction of

the peak strain values and a better simulation of the experimental results is observed (especially for the case of gauge 2).

Fig. 18 shows, for a DST-1w-like specimen and for each of the abovementioned models, the axial stress distributions within the laminate at the end of the numerical analyses, i.e. under the imposed displacement of 35 mm; the numerical simulation was always carried out by assuming  $G_f = 5$  GPa. In particular, Fig. 18a refers to model 1, Fig. 18b to model 2 and Fig. 18c to model 3; of course, Fig. 18b and c gives rise to the same axial stress regime.

These plots give an idea about relevant aspects, such as the stress concentration developing around the fastener location, the entity of such stress values, the stress components (tension “+” or compression “-”), the width of the FRP area involved by this stress concentration.

Fig. 19a and b shows the results of simulations performed through SAP2000 for a DST-4Aw-like specimen.

In particular, the figures depict the comparison between the experimental strain values measured during the test DST-4Aw(c) by strain gauges 1, 2, and 3 (see the schematic of Fig. 19c), and the numerical ones. Also in this case, the analytical simulations were performed by using models 1, 2 and 3 and by both considering  $G_f = 3$  GPa and  $G_f = 5$  GPa (Fig. 19a and b, respectively). The

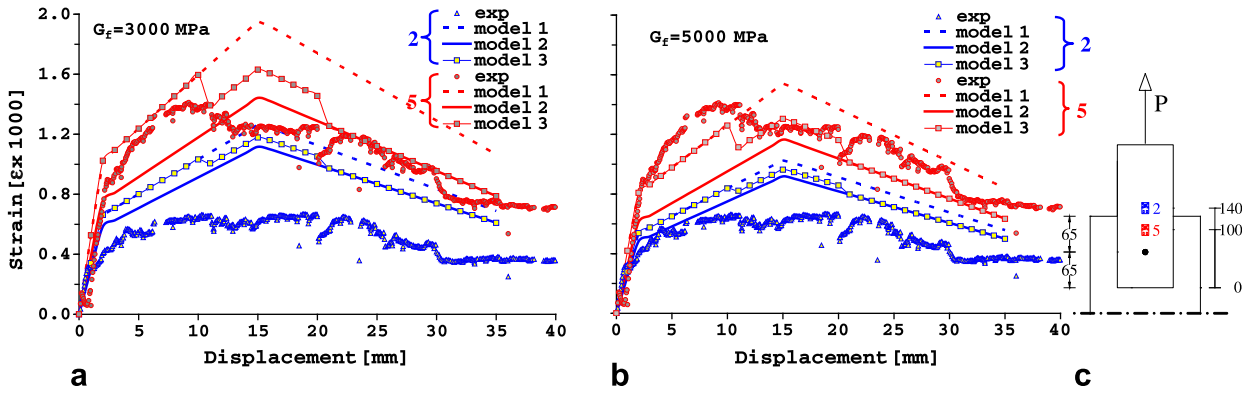


Fig. 17. Comparison between numerical and experimental strain values: test DST-1w(c).

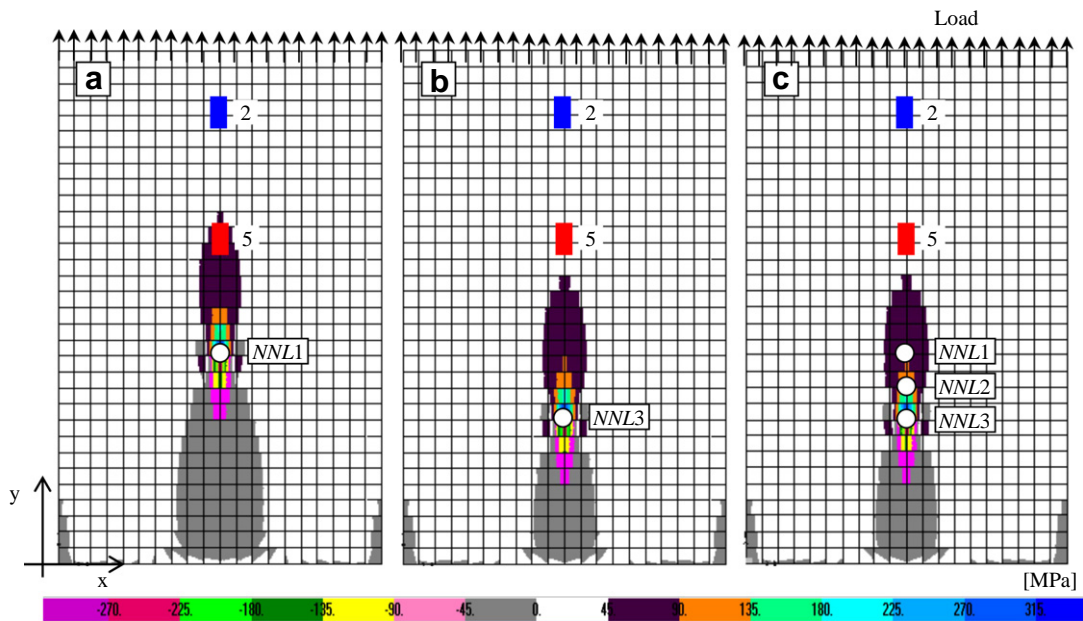


Fig. 18. Numerical simulation of the axial stress distribution within the FRP laminate ( $G_f = 5000$  MPa): DST-1w test series.

gauge 4, also shown in Fig. 19c, stopped working prematurely during the test, and the related experimental readings are missing in the comparisons.

The figures show that the initial slope of the experimental curves is always lower than that obtained by numerical simulations; this mismatch might be attributed to the analytical modeling that does not account for any possible initial slip occurring in the experimental test when fasteners are not perfectly tightened inside the laminate and, therefore, a gap between holes and screws is experienced.

Regardless of the model used for the numerical simulations, the shear modulus does not significantly affect the strain/stress regime as differently observed for DST-1w specimens; however, in the DST-4Aw specimens, the strain gauges are always placed on the mid-width of the laminate and, therefore, are not aligned with the fasteners location where the influence of the shear modulus on the stress/strain distribution may result significant.

The experimental–numerical comparisons also highlight that all the considered models give rise to accurate simulations, although the model 3 generally performs better than the others.

For this reason, Fig. 19d and e shows the further comparison between the strain data measured during test DST-4Aw(b) by gauges

2, 3 and 4 (strain gauge 1 did not work properly) and the numerical ones obtained by implementing the model 3; the very good agreement between numerical and experimental results can be observed from these figures.

Fig. 20, instead, shows the axial stress distribution obtained for a DST-4Aw-like specimen, under an imposed displacement of 30 mm and by considering  $G_f = 5$  GPa. The two stress diagrams correspond to position “i” (model 1 in Fig. 20a) and “f” (model 2 in Fig. 20b) of the fastener, respectively, whereas the stress distribution obtained by considering model 3 is not reported since it obviously coincides with that of the model 2.

The overlap of the four strain gauge positions on the two stress diagrams is useful for better understanding how the movement of the NLL element from the initial to the final position can affect the stress distribution in the area around the fastener and, consequently, the entity of the numerical strain values (i.e. those shown in Fig. 19).

The accuracy of FEM models can be finally pointed out from Fig. 21, where the experimental load–slip ( $H-s_f$ ) relationships of all DST-1w and DST-4Aw test specimens (Fig. 21a and b, respectively) are compared with the corresponding numerical simulations obtained by implementing each of the considered models.

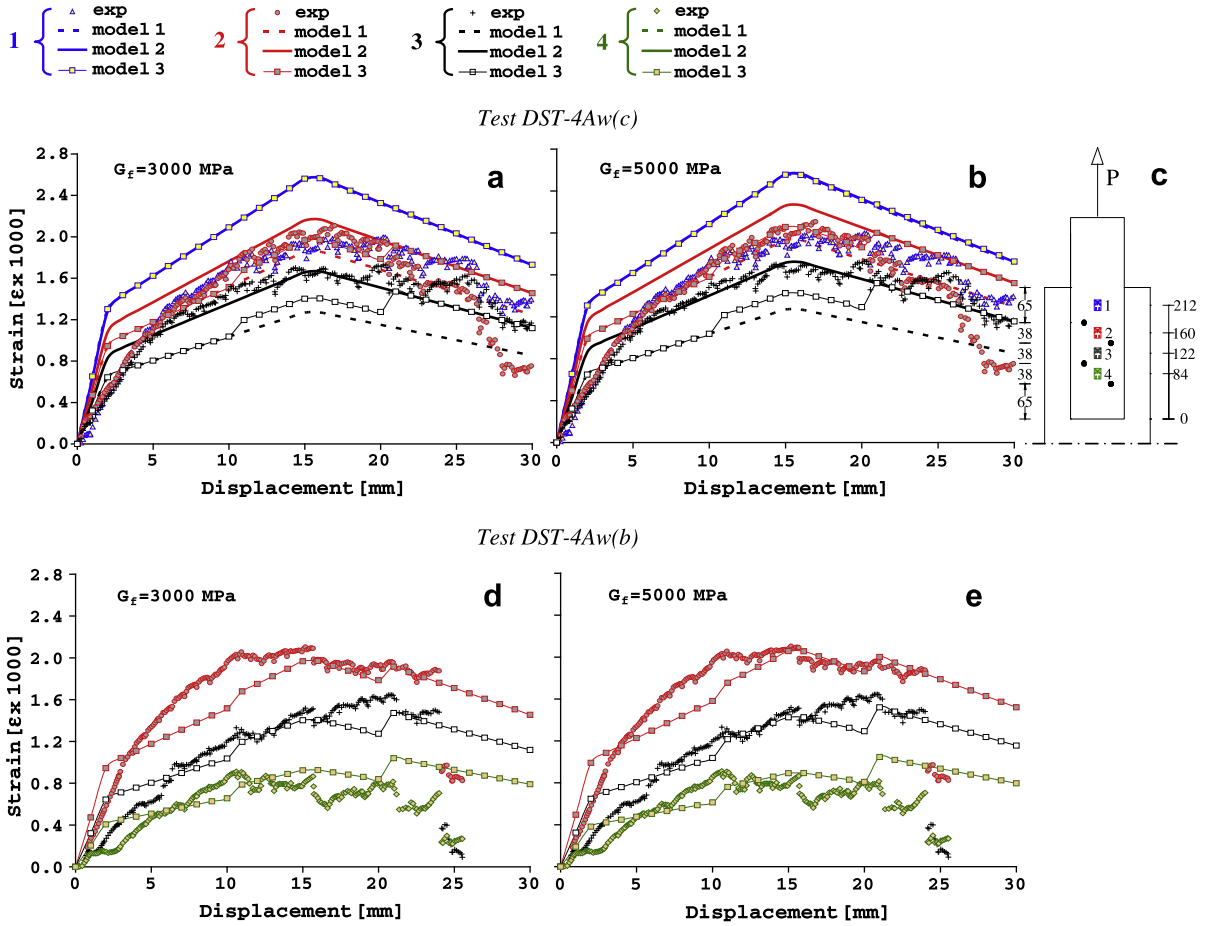


Fig. 19. Comparison between numerical and experimental strain values: test DST-4Aw(c) and DST-4Aw (b).

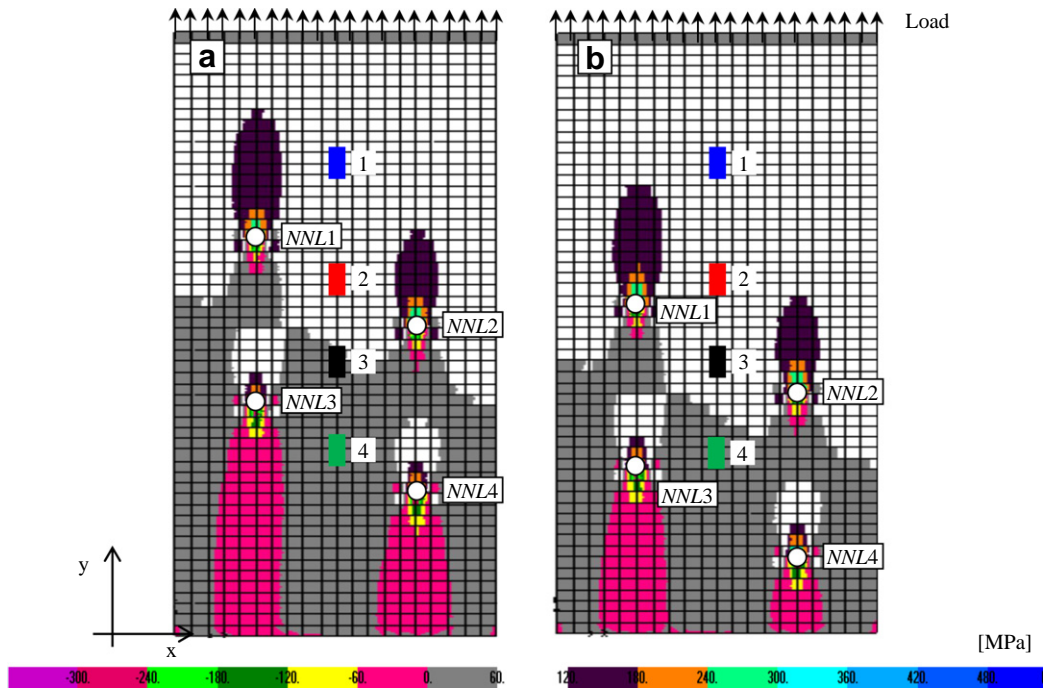


Fig. 20. Numerical simulation of the axial stress distribution within the FRP laminate ( $G_f = 5000$  MPa): DST-4Aw test series.

As observed, the three numerical curves overlap each other perfectly, thus showing that the models influence in a different

way the local response of the connection but not the simulation of the global performance. For the same reason, the variability of

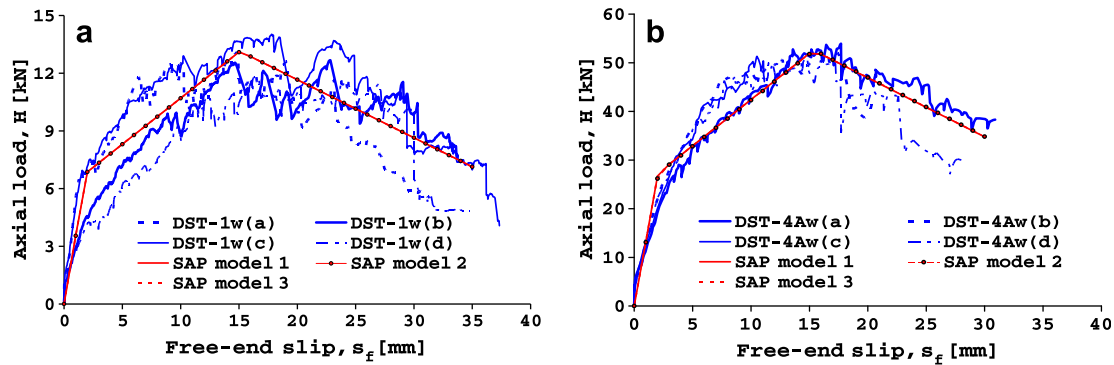


Fig. 21.  $H$ – $s_f$  experimental–numerical comparisons: DST-1w test series (a); DST-4Aw test series (b).

the shear modulus  $G_f$  was disregarded in the simulation of the experimental  $H$ – $s_f$  responses, and the numerical results obtained by only considering  $G_f = 5$  GPa are shown.

## 6. Conclusions

This paper presented the results of numerous direct shear tests performed on FRP laminates mechanically fastened to concrete prisms; the tested specimens were realised by employing a normal strength concrete and a variable number of steel screws.

The experimental results pointed out relevant information about the influence on the force–slip response of MF-FRP laminates of fastener detailing, number and pattern of anchors.

Disregarding the influence of fastener layout, it has been shown that the force–displacement curves obtained from connections with fasteners without washer are affected by a significant level of variability even in the case of similar specimens; the post peak response is characterized by a remarkable softening branch which early leads to a faster achievement of the conventional collapse.

Conversely, FRP laminates fastened using washers exhibited a more regular behavior with higher displacement values achieved at collapse; moreover, the peak strength of the connection almost doubled as the number of fastener was increased from 2 to 4.

It has also been shown that the fastener spacing plays a more relevant role in the case of tests w/o washer where a better performance of the connection is generally associated to anchors with larger spacing.

Simplified finite element models were then implemented in SAP2000 for simulating the behavior experimentally observed and investigating the effect induced by staggered anchor patterns on the axial stress regime. In particular, in order to simulate the effect of the relative laminate–anchor displacement, three alternative models were studied and their efficacy in simulating the experimental behavior was investigated.

The numerical modeling also provided useful information about the influence of the shear modulus on the strain/stress regime developing within the FRP laminate.

Although more sophisticated models are needed, the numerical simulations have shown that in the case of tests with one fastener, the strain distribution within the laminate significantly relies on the value of  $G_f$ ; however, this was not fully confirmed in the case of tests with multiple fasteners where only a slight influence was observed.

## Acknowledgment

The authors acknowledge the financial support provided by ReLUIS for the research program funded by the Department of Civil Protection – Executive Project 2010–2013.

The authors gratefully acknowledge *Fidia s.r.l.* (Perugia, Italy) for supplying the MF-FRP laminates employed in the experimental campaign.

## References

- [1] Lamanna AJ. Flexural strengthening of reinforced concrete beams with mechanically fastened fiber reinforced polymer strips. Ph.D. thesis, University of Wisconsin–Madison, USA; 2002. p. 1–287.
- [2] Lamanna AJ, Bank LC, Scott DW. Flexural strengthening of reinforced concrete beams using fasteners and fiber reinforced polymer strips. *ACI Struct J* 2001;98(3):368–76.
- [3] Lamanna AJ, Bank LC, Scott DW. Flexural strengthening of reinforced concrete beams by mechanically attaching fiber-reinforced polymer strips. *J Compos Construct* 2004;8(3):203–10.
- [4] Oliva M, Bank LC, Borowicz DT, Arora D. Rapid strengthening of reinforced concrete bridges. Technical report, University of Wisconsin Madison, Wisconsin Highway Research Program, USA; 2003. p. 1–167.
- [5] Rizzo A. Application of mechanically fastened FRP (MF-FRP) pre-cured laminates in off-system bridges. M.Sc. thesis, University of Missouri-Rolla, USA; 2005. p. 1–285.
- [6] Lamanna AJ, Bank LC, Borowicz DT. Mechanically fastened FRP strengthening of large scale RC bridge T beams. *Adv Struct Eng* 2004;7(6):525–38.
- [7] Martin JA, Lamanna AJ. Performance of mechanically fastened FRP strengthened concrete beams in flexure. *J Compos Construct* 2008;12(3):257–65.
- [8] Napoli A. RC structures strengthened with mechanically fastened FRP systems. M.S. thesis University of Miami, USA; 2008. p. 1–78.
- [9] Lee HL, Lopez MM, Bakis CE. Flexural behavior of reinforced concrete beams strengthened with mechanically fastened FRP strip. In: *Proceedings of FRPRCS-8*. Patras, Greece, July 2007. p. 1–9.
- [10] Brown VL, Bank LC, Arora D, Borowicz DT, Godat A, Lamanna AJ, et al. Experimental studies of mechanically-fastened FRP systems: state-of-the-art. ACI special publication – *Proceedings of the FRPRCS-10*. Tampa Bay, FL, USA, April 2011.
- [11] Quattlebaum JB, Harries KA, Petrou MF. Comparison of three flexural retrofit systems under monotonic and fatigue loads. *J Bridge Eng* 2005;10(6):731–40.
- [12] Ekenel M, Rizzo A, Myers JJ, Nanni A. Flexural fatigue behavior of reinforced concrete beams strengthened with FRP fabric and precured laminate systems. *J Compos Construct* 2006;10(5):433–42.
- [13] Sena-Cruz JM, Barros JAO, Coelho MRF, Silva LFFT. Efficiency of different techniques in flexural strengthening of RC beams under monotonic and fatigue loading. *Constr Build Mater* 2011;29:175–82.
- [14] Ebead U. Hybrid externally bonded/mechanically fastened fiber-reinforced polymer for RC beam strengthening. *ACI Struct J* 2011;108(6):669–78.
- [15] Johnson D. An investigation for strengthening existing reinforced concrete beams in shear using a MF-FRP retrofit system. Master thesis, University of Wisconsin-Madison, USA; 2011. p. 1–202.
- [16] Elsayed WE, Ebead UA, Neale KW. Mechanically fastened FRP-strengthened two-way concrete slabs with and without cutouts. *J Composites Construct* 2009;13(1):198–207.
- [17] Dempsey DD, Scott DW. Wood members strengthened with mechanically fastened FRP strips. *J Compos Construct* 2006;10(5):392–8.
- [18] Ascione L, Napoli A, Realfonzo R, Matta F, Nanni A. Strengthening of masonry with mechanically fastened FRP laminates. In: *Proceedings of MuRiCO3 “Mechanics of Masonry Structures strengthened with Composite Materials”*. Venice, April, 2009.
- [19] Bank LC, Arora D. Analysis of RC beams strengthened with mechanically fastened FRP (MF-FRP) strips. *Compos Struct* 2007;79(2):180–91.
- [20] Napoli A, Matta F, Martinelli E, Nanni A, Realfonzo R. Modeling and verification of response of RC slabs strengthened in flexure with mechanically fastened FRP laminates. *Mag Concr Res* 2010;62(8):593–605.

- [21] Martinelli E, Napoli A, Realfonzo R. Interfacial behavior between Mechanically Fastened FRP laminates and concrete substrate. In: Proceedings of CICE 2010, Beijing (China); 2010. Paper 194.
- [22] Lee JH, Lopez MM, Bakis CE. Slip effects in reinforced concrete beams with mechanically fastened FRP strip. *Cem Concr Compos* 2009;31(7):496–504.
- [23] Faella C, Martinelli E, Nigro E. Formulation and validation of a theoretical model for intermediate debonding in FRP-strengthened RC beams. *Compos Part B: Eng.* 2008;39(4):645–55.
- [24] Elsayed WE, Ebead UA, Neale KW. Studies on mechanically fastened fiber-reinforced polymer strengthening system. *ACI Struct J* 2009;106(1):49–59.
- [25] SAP2000 structural analysis program. Computer and structures, Inc., Berkeley, CA. Version 14; 1995.
- [26] Strongwell, <<http://www.strongwell.com>>; 2010 [accessed 09.14.10].
- [27] Rizzo A, Galati N, Nanni A, Dharan LR. Material characterization of FRP precured laminates used in the mechanically fastened FRP strengthening of RC structures. In: Proceedings of FRPRCS-7, SP-230–8, American Concrete Institute. 2005; 230: 135–152.
- [28] Hilti: Universal Screw Anchor, <<http://www.us.hilti.com/holus>>; 2010 [accessed 09.14.10].
- [29] Kelly G, Hallstrom S. Bearing strength of carbon fibre/epoxy laminates: effects of bolt-hole clearance. *Composites Part B* 2004;35:331–43.
- [30] Faella C, Martinelli E, Nigro E. Direct versus indirect method for identifying FRP-to-concrete interface relationships. *J Compos Construct* 2008;13(3): 226–33.
- [31] Martinelli E, Napoli A, Nunziata B, Realfonzo R. FRP laminates mechanically fastened to concrete: experimental observations and numerical modeling. In: Proceedings of SMAR2011. Dubai, UAE, February 2011.
- [32] Martinelli E, Napoli A, Nunziata B, Realfonzo R. Inverse identification of a bearing-stress-interface-slip relationship in mechanically fastened FRP laminates. *Compo Struct.* 2012;94(8):2548–60.